LOW-CYCLE FATIGUE BY CONSTANT AMPLITUDE TRUE MEAN STRESS*

By

L. GILLEMOT

Department of Mechanical Technology, Polytechnical University, Budapest

(Received December 28, 1965)

The absorbed energy per unit volume necessary for the fracture consists of three parts: the energy of elastic deformation, the energy of plastic deformation and the energy necessary for crack spreading. In the case of the simple tensile test the energy necessary for crack spreading is negligible.

It was supposed earlier that the energy necessary for fracture is independent from the lattice defects, at least in first approximation. This would mean, therefore, that the energy necessary for the appearance of the first spreading crack is of a constant value. In order to prove this supposal, low-cycle fatigue tests have been carried out at constant true mean stress amplitude. It was found that the absorbed energy per unit volume absorbed before the appearance of the spreading crack has always the same value independent from the stress level. The energy determined by low-cycle fatigue agrees within the limits of scatter with the energy measured by the tensile tests.

1. Introduction

Phenomena and regularities encountered in course of low-cycle fatigue are dealt with by extensive literature. The great number of publications has been reviewed by several authors [1, 2, 3] in recent times through comprehensive studies. The majority of these publications explain either constant load amplitude fatigue or constant strain amplitude fatigue. Relatively few experiments have been performed on true stress amplitude fatigue [4]. As far as practical applications are concerned, only either constant load amplitude experiments or constant strain amplitude experiments are, naturally, of any significance. Experiments on constant true strain amplitude are rather interesting only from theoretical aspects as by their means the mechanism of fracture can be studied.

* Delivered and published at the International Conference on Fracture, Sendai (Japan) Sept. 1965.

In course of experiments conducted with constant strain amplitude a correlation between the total plastic true strain of the sample and its total elongation as determined under tension test conditions could be established [5, 6, 7, 8]. Accordingly,

$$N^m \cdot \varepsilon_p = c \tag{1}$$

COFFIN et al. claim a value of $^1/_2$ for exponent m. Assuming the static tensile test conforming to $N = {}^1/_4$ cycle, and a true strain of ε_f at fracture as measured under static tensile conditions, then the value of constant c would amount to $\frac{\varepsilon_f}{2}$ where ε_f may be determined from the reduction of area (R) value:

$$\varepsilon_f = \ln \frac{1}{1 - R} \tag{2}$$

Subsequently, elongation and/or reduction of area values are always expressed as absolute figures instead of percentages and, furthermore, true elongation always represents the local elongation determined by the minimum cross-section of the sample, thus

$$\varepsilon = \ln \frac{A_0}{A}$$

where A_0 is the initial cross-section, while A represents the minimum modified cross-section value. Identically, normal or engineering strain means

$$\delta = \frac{L_1 - L_0}{L_0} = \frac{A_0}{A} - 1$$

Equation (1) developed entirely empirically has been supported recently by statistical considerations by GITTUS [9] as well as by physical findings by GILMAN [10].

Theoretically, it may be assumed that the true strain pertaining to the $N = {}^1/_2 - {}^1/_4$ load under true stress amplitude experiment conditions would appear identical to the true fracture stress determined under tensile test conditions [11, 3].

Literature refers to a number of publications where the energy absorbed by the sample is indicated as the criterion of fracture [12, 13, 14]. FELTNER and MORROW [14] assumed that the energy absorbed during the fatigue process was identical to the energy absorbed in course of the static tensile test.

Our experiments aimed at discovering by means of low-cycle fatigue tests performed with true stress amplitude, the correlation existing between

the energy absorbed per unit volume during the static tensile test and the energy absorbed under fatigue test conditions and at verifying that the terminal of the curve $S - N$ plotted in true stress coordinates is, at a load of $N = {}^1/_2 - {}^1/_4$, identical to the true fracture stress.

The comparison of tensile test data to low-cycle fatigue data, however, may only be accurate with an identical strain velocity as both the tensile test results and fatigue test results are affected by the strain rate.

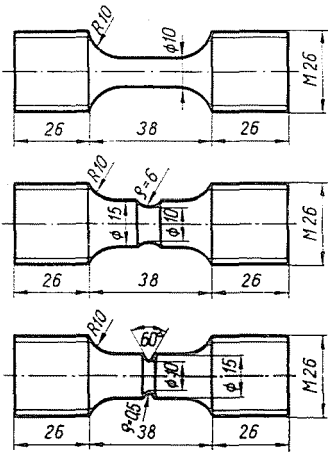

Fig. 1. Samples used for low-cycle fatigue test purposes

Several authors (e.g. [6, 15]) discovered that fatigue strength decreases with the decreasing cycle rate. In our experiments, therefore, a constant strain rate of $U = 2$ mm/min has been employed and the fatigue tests have been performed also by applying the same rate.

For this purpose, samples have been produced of 0.35% *C*-content carbon steel water-quenched at 860 °C and annealed for 1 hour at 600 °C. For these experiments unnotched cylindrical samples of 10 mm diameter and 25 mm gauge length have been made use of as well as notched ones of 15 mm unnotched and 10 mm notched diameters. The bend radii of notchings amounted to 6 mm for one sample type and to 0.5 mm for the other. With these figures the stress concentration factors of the two notched sample types have been within the elastic range 1.32 and 3.05 resp. *(Fig.1)*.

For these experiments a very hard tensile machine having a spring constant of $f = 10^4$ kp/mm was used, as, according to the results of preliminary experiments, instrument rigidity affects measurement data to a significant extent.

In the compression phase a separate device was employed to prevent sample deflection.

2. Strain rate variation during the tensile test

In course of the tensile test strain rate will stay constant only until elongation will stay uniform. Under necking conditions elongation rate will greatly vary. According to the experiments by CZOBOLY [16], there may be three phases distinguished within the tensile test *(Fig. 2)*. The figure presents the extension of the sample as measured on the vertical axis in mm. The horizontal axis represents the reduction of area as determined by the minimum cross-section. In the first phase, sample elongation appears uniform covering

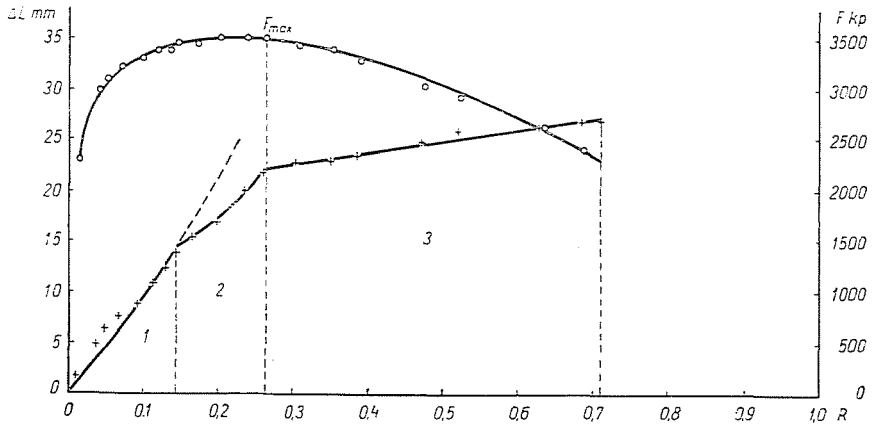

Fig. 2. Force and elongation variations in function of the reduction of area (low-carbon steel C-15)

the entire length of the sample whereas in the third phase there is only a local contraction to be observed. In the intermediate phase joint local contraction and elongation involving the total sample length take place. The vertical axis of *Fig. 1* has the force variation also plotted. Maximum force (F_{max}) is produced within the second phase coinciding, generally, with its terminal. With the force decreasing (in the third phase), lengthening due to contraction is proportional to area reduction, thus

$$\Delta L = k \cdot d_0 \cdot (R - R_m) \tag{3}$$

where d_0 is the sample diameter, k represents a proportion factor being for cubic lattice metal types equal to 1 and R_m means the reduction of area caused by maximum force effect. With an extremely hard tensile test machine, chuck displacement in the third phase is exactly equal to the elongation given by equation (3). Differentiating equation (3) by time

$$\frac{d(\Delta L)}{dt} = k \cdot d_0 \cdot \frac{dR}{dt} = U \tag{4}$$

According to the law of constancy of volume:

$$1 + \delta = \frac{1}{1 - R} \tag{5}$$

Differentiating equation (5) by time and substituting from equation (4) strain rate is:

$$c = \frac{d\delta}{dt} = \frac{1}{(1 - R)^2} \cdot \frac{dR}{dt} = \frac{1}{(1 - R)^2} \cdot \frac{U}{k \cdot d_0} \tag{6}$$

As equation (6) reveals, the strain rate is rapidly increasing with the increasing reduction of area even with a constant elongation rate (U). Due to the specific elongation rate varying under necking condition, the force value will similarly vary. The strain rate effect has been expressed on grounds of theoretical considerations by the following equation by PRANDTL [17]:

$$F_1 = F_0 + m \cdot \ln \frac{c_1}{c_0} \tag{7}$$

According to the PRANDTL equation specific elongation rate corresponds to force F_1 whereas elongation rate c_0 to force F_0. Dividing equation (7) by cross-section A_m developed by the maximum force

$$S_{m1} = S_{m0} + a \cdot \ln \frac{c_1}{c_0} \tag{8}$$

The value of constant a as calculated from the data rendered by [18, 19 and 20] will amount to 1.2 kp/mm^2 for copper, 4.5 kp/mm^2 for mild steel types and 1 kp/mm^2 for aluminium if, instead of the log. nat. in equation (8), common (Briggsian) logarithm is being made use of in calculations. According to the results of experiments hitherto conducted, the value of constant a is hardly affected by alloying [21].

Dividing equation (7) by an optional cross-section A, the equation of the true stress—true strain curve may be written as follows:

$$S_1 = S_0 + a \cdot \frac{1 - R_m}{1 - R} \cdot \ln \frac{c_1}{c_0} \tag{9}$$

Equation (9) permits in general the composition of the true stress curve equation [22] as at the beginning of contraction $R = R_m$ with c_0 representing the elongation rate necking is being started with:

$$c_0 = \frac{1}{(1 - R_m)^2} \cdot \frac{U}{k \cdot d_0} \tag{10}$$

thus

$$s_1 = s_0 + a \cdot \frac{1 - R_m}{1 - R} \cdot \ln \left(\frac{1 - R_m}{1 - R} \right)^2 \tag{11}$$

This equation describes the true stress—true strain diagram with a great accuracy [22].

If, therefore, the fracture stress as determined by the measurement amounts in the moment of fracture to S_{1f}, then the fracture stress S_{0f} pertaining to the constant elongation rate can be determined by means of equation (11). The second term of the equation expressing rate effect is, for material

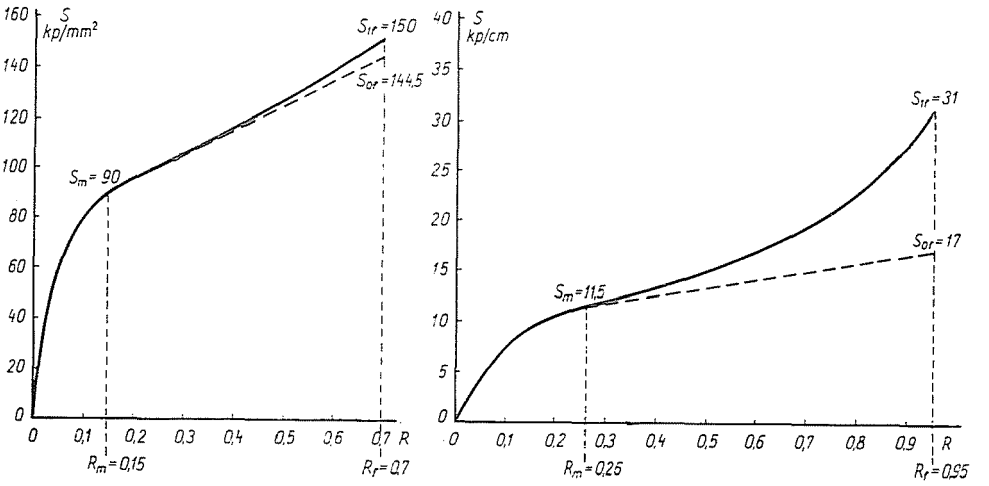

Fig. 3. True stress—true strain diagram of a quenched and tempered carbon steel (a). and of a 99.99% pure aluminium (b)
Full Line: $U = 2$ mm/min
Dashed line: strain rate, c = constant

types of lesser reduction of area, not very significant as, for example, in case of a steel type where $S_{1f} = 150$ kp/mm², $R_m = 0.15$ and $R_f = 0.7$, the S_{0f} value as determined by means of equation (11) will differ from the measured S_{1f} value by not more than 5.5 kp/mm² *(Fig. 3a)*. However, in case of material types of great reduction of area such as, for example, pure aluminium *(Fig. 3b)*, the measured value of S_{1f} is 31 kp/mm² whereas S_{0f} as calculated from equation (11) only 17 kp/mm² [21, 22].

It is seen, therefore, that in case of material types of great reduction of area the elongation rate variation during contraction can affect fracture stress value, while for material types of lesser contraction the elongation rate effect is negligible. In case of great reduction of area substances it ought to be taken into consideration that the stress distribution is not uniform all over the cross-section [23, 24, 25] but the peak stress produced along the centre line of the sample exceeds the true mean rupture stress value.

3. Low-cycle fatigue tests with constant true stress amplitude

The low-cycle fatigue test has been performed by using unnotched as well as notched samples of the two specified types in case of the latter. Since the loading rate applied in these experiments was identical to the rate employed in course of the tensile test, the experiments have been carried out only up to a very low cycle number. Accordingly, the alternating true stress amplitude appeared relatively high. Experiments have been performed with alternating true mean stresses of $S = 72.5$, 75, 85, 88, 95, 100 and 104 kp/mm², respec-

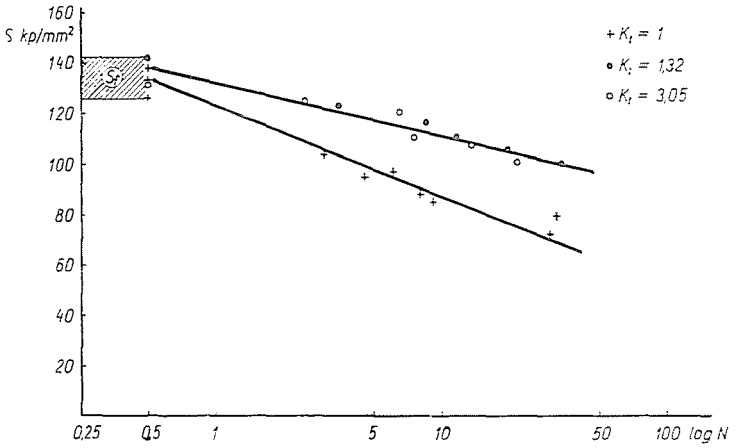

Fig. 4. $S-N$ curve of unnotched and notched samples, resp.

tively. On grounds of the data rendered by a number of tensile tests, the true stress pertaining to the maximum force could be found as $S_m = 89-95$ kp/mm², true mean fracture stress as $S_f = 122-138$ kp/mm², and the true fracture strain as $\varepsilon_f = 0.94-1.02$. Some of the stress levels employed in course of low-cycle fatigue appeared lower than S_m causing, consequently, only a uniform elongation due to the first loading whereas, at stress levels exceeding S_m, contraction took place as soon as upon the first tension. The experimental results are illustrated by *Fig. 4*. The horizontal axis presents the number of reversals while the vertical one has the true stress plotted. The points shown by both unnotched and notched samples are located on a straight line coinciding, at the load figure $N = {}^1/_2-{}^1/_4$ and within the margin of error, most precisely with the true fracture stress S_f determined by the static tensile test.

Suggestions differ whether the tensile test results should be taken into consideration on grounds of $N = {}^1/_2$ or ${}^1/_4$. Essentially, however, the findings are not affected by this problem.

It seems remarkable that the line of both unnotched and notched samples terminates with an identical S_f value. This is in full agreement with the claim

by LUDWIK according to which the fracture stress value determined by the tensile test is independent of notching. However, this finding by LUDWIK is only true if the notched diameter of the samples compared is identical. The fracture stress of notched samples of different notched diameters made, however, of identical material may greatly vary [23]. This is why samples of identical notched diameter have been used in the experiments referred to.

4. Absorbed energy per unit volume

The absorbed energy per unit volume is, in course of the tensile test,

$$W = \int \frac{F \cdot dL}{V} = \int \frac{F \cdot dL}{A \cdot L} = \int s \cdot d\varepsilon \tag{12}$$

where V represents an infinitesimal volume selected within the cross-section of the fracture. This is nothing else but the area enclosed by the true stress — true strain diagram.

By calculating the integral, this work can be determined by means of the strength characteristics usually employed in material testing [26, 27]. The total energy required to produce fracture consists of three phases: that for elastic deformation W_e, for plastic deformation W_p, and the energy required during crack propagation (W_c). With a sufficiently considerable plastic deformation, the energy required for elastic deformation and crack propagation is, in tensile test, negligible as compared to that necessitated by the plastic deformation, that is, $W \cong W_p$.

Subsequently, it will be verified that the specific energy produced up to the moment of fracture is not structure sensitive, that is, it does not depend on lattice defects in practice.

The strength of metal types without lattice defects has been first estimated by OROWAN [28] and POLÁNYI [29], respectively. OROWAN assumed that the elastic deformation energy in perfect lattice whiskers is equal to the energy of the surfaces developed following fracture. In his calculations, for simplicity's sake, interatomic force variations have been supposed to represent a sinusoid curve. According to OROWAN, the perfect lattice crystal strength is expressed by the following formula:

$$S_t = \sqrt{\frac{E \cdot \gamma}{d}} \tag{13}$$

where E represents Young's modulus,
γ is the surface energy per unit area, and
d is the distance of the atomic planes.

Recently, some more detailed calculations revealed [30] that the values obtained by using the OROWAN formula are somewhat high. The true situation is further approximated by the formula suggested by POLÁNYI, according to which

$$S_t = \frac{2\gamma}{d} \tag{14}$$

Assuming that the energy absorbed in course of the plastic deformation of very pure metals is identical to that absorbed by perfect lattice whiskers up the moment of fracture, a relation may be arrived at [31], according to which

$$S_t = \sqrt{\frac{W \cdot E}{2}} \tag{15}$$

Equation (15) represents only a crude approximation but more accurate calculations would also affect only the constant value.*

In order to verify the independence of specific fracture energy of lattice defects, the energy absorbed during the tensile test by spectroscopically pure silver, aluminium, copper, iron and nickel, respectively, has been determined. Calculating from these data by means of equation (15), the strength (S_t) of perfect lattice whiskers, a very good agreement could be discovered with either the values calculated by means of equation (14) from the surface energy data or those hitherto measured [32] for whiskers. The results are shown by *Table I*. Figures in the first column of the Table are calculated from the surface energy measured in liquid metal phase by making use of equation (14). Data in the second column are rendered, similarly on the basis of equation (14), by surface energy figures obtained in solid state [33]. The third column presents strength values as measured in whiskers according to [32] while the figures in column IV are calculated by means of equation (15) from data on plastic deformation

Table I

Strength of perfect lattices. S_t kp/mm²

Material	I	II	III	IV
Ag	656	—	176	692
Al	372	450	—	420
Cu	885	805	900 300	800
Fe	1200	1350	1340	1320
Ni	—	1070	—	1030

* The more accurate calculations referred to will be published later.

energy absorbed up to fracture. The agreement among data determined by different methods appears very satisfactory and, therefore, it seems justified to assume that the plastic deformation energy absorbed up to fracture represents a lattice characteristic independent, in first approximation, of lattice defects. It may be assumed, furthermore, that a crack spreading upon the effect of a mechanism not being dealt with here would be started by the lattice defects in the material only in such cases when the energy absorbed in course of plastic deformation has reached a value characteristic to the respective material.

5. Energy absorbed in low-cycle fatigue process

According to the findings by COFFIN et al., the $\varepsilon - N$ curve of low-cycle fatigue performed with constant strain amplitude terminates in the ε_f value determined by the static test. However, according to our previous statement, the $S - N$ curve of experiments carried out with constant true stress amplitude will terminate in the true fracture stress value S_f determined by the tensile test and defined above. These two discoveries lead to the conclusion that the fatigue process, at least up to the appearance of the first crack, is governed by the energy absorbed in course of the process proper.

The statement introduced in Paragraph 4, according to which, in case of extremely pure metals, the energy absorbed up to whisker fracture is identical to the plastic deformation energy measured in the annealed polycrystalline state of the respective metal leads to the conclusion that the absorbed energy per unit volume is not structure sensitive. It follows that the process of fracture consists of two phases: one is the plastic deformation work represented by a value characteristic to the given metal or alloy, and the other is the work required for crack spreading.

To explain these, the plastic deformation taken place as well as the absorbed energy per unit volume have been determined in each cycle of the low-cycle fatigue experiments. As emphasized earlier, true strain was determined by means of diameter measurements so as to always represent the true strain produced within the minimum cross-section of the sample. Some examples of the measurement results are illustrated by *Figures 5* and *6*. The horizontal axis of each figure presents the number of loadings whereas the vertical one the true strain, that is, the specific energy produced up to the respective cycle number. Due to experimental difficulties, the constant true stress could not be adjusted accurately in each cycle. For cycles where, due to experimental difficulties, a true stress value other than the projected one has been obtained, the figure adjacent to the true strain curve represents the true stress value actually arrived at. Apart from these exceptions, projected true stresses could be adjusted with an accuracy of $\pm$ 1 kp/mm^2.

Fig. 5 presents the results of experiments performed with a stress of $S = 72$ kp/mm². Up to the twelfth repetition, the true strain exhibits an increasing trend both at the tension and compression sides with the exception of the short initial section of the compression side where the initial decreasing trend may be traced back to the true stress of 75 kp/mm². Subsequent to the twelfth loading, the character of the curve is obviously changed and between the fifteenth and sixteenth loadings there is a visually perceptible large crack observed to have developed. It seems justified to assume that the modification

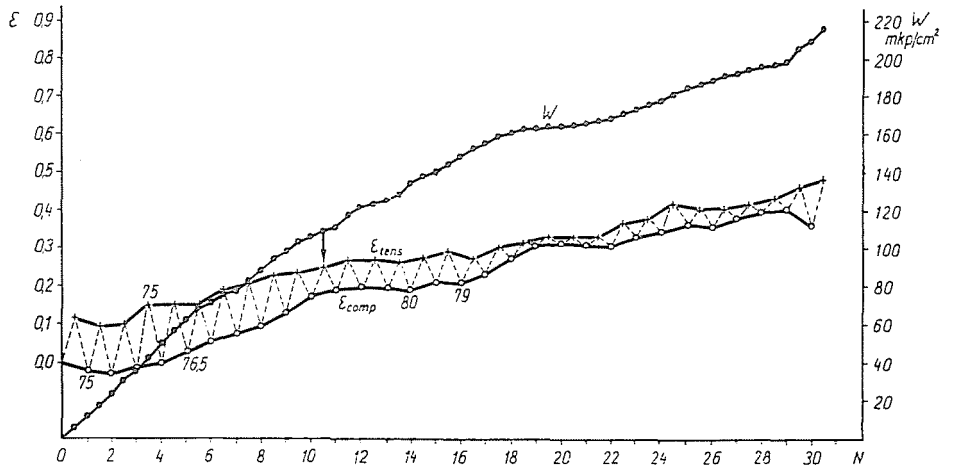

Fig. 5. True strain and absorbed energy variations in function of the cycle number ($S = 72$ kp/mm²)

of the strain curve character may be attributed to the effect of the first spreading crack. Following the appearance of the crack, at least in each tension period, the sample will exhibit a notched behaviour with its true strain decreasing by each period of tension whereas the crack would exert an evidently lesser influence on plastic deformation in each compressing period.

A similar phenomenon is illustrated although more markedly by the test performed with a true stress of $S = 90$ kp/mm² *(Fig. 6)*. The crack grew visible here as soon as by the fourth tension and, from then on, the true strain displayed on the tension side a decreasing trend all along.

The true strain curve modification coincided, in each test, to a good accuracy with the specific absorbed energy of 100 to 120 mkp/cm³. The figures have an arrow indicating the absorbed energy value corresponding to 110 mkp/cm³. As revealed by *Figures 5* and *6*, it is the specific energy value determined by the simple tensile test, within the margin of error where the character of the process will be modified from. The difference between the two characteristic curves introduced by *Figures 5* and *6* may be explained by the fact that, in course of the test performed with a true stress of 90 kp/mm², a con-

siderable contraction took place as soon as upon the first loading and the contraction of the sample has increased, up to the absorption of 110 mkp/cm^3 energy, to a considerable extent whereas in experiments conducted with a true stress of $S = 72$ kp/mm^2 the crack appeared in an early phase of the necking.

The appearance of the crack coincided in each test with the value of the 110 mkp/cm^3 total energy consumed which represented the value characteristic to the material tested. The energy produced in course of the spreading

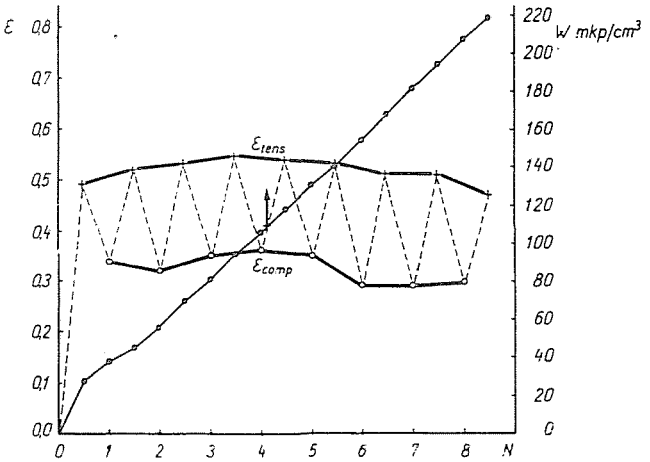

Fig. 6. True strain and absorbed energy variations in function of the cycle number ($S = 90$ kp/mm^2)

of a crack depends, to a great extent, on the stress level. The lower the stress level fatigue has been effected at, the more energy had to be consumed to spread the crack. While the energy consumed up to the appearance of the first crack represented, within a range of $\pm$ 10 per cent, an identical quantitative value in all cases, the nature of the energy consumed to spread the crack as increasing with the reduced stress level could be unequivocally recognized but this exhibited a considerable standard deviation. In experiments repeated at an identical stress level, the energy produced up to the appearance of the spreading crack amounted in each case to 110 $\pm$ 10 mkp/cm^3 whereas the energies measured in course of the spreading of the crack revealed, even at identical stress levels, a fluctuation of 20 to 40 per cent. Due to experimental difficulties and to the slowness of the test, there is an insufficient number of data available, as yet, to permit arriving at an unequivocal conclusion concerning the energy required for crack spreading. It seems, however, absolutely obvious that the energy required for the spreading of a crack although correlated to the macroscopic characteristics of the material is greatly influenced by local inhomogeneities.

Fig. 7 has the number of loadings indicated, on the curve S—N measured for unnotched samples, whence the subsequent fracture process was governed by the extension of the crack. The measurement points are located, in the coordinate system S — log$N$, with rather considerable accuracy along a straight

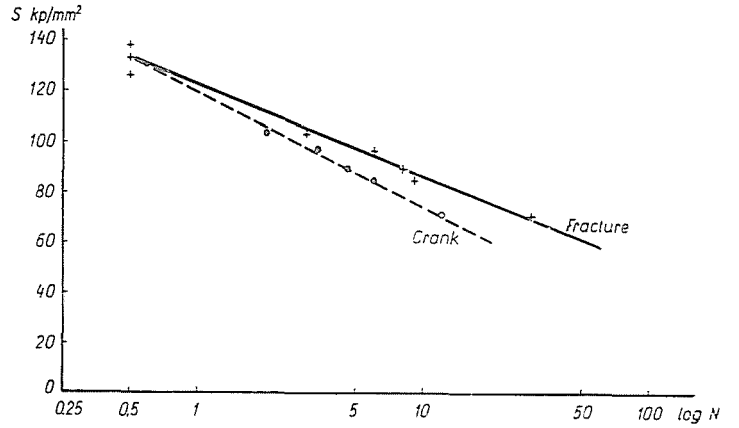

Fig. 7. Load number resulting in a spreading crack (dashed line) and/or fracture

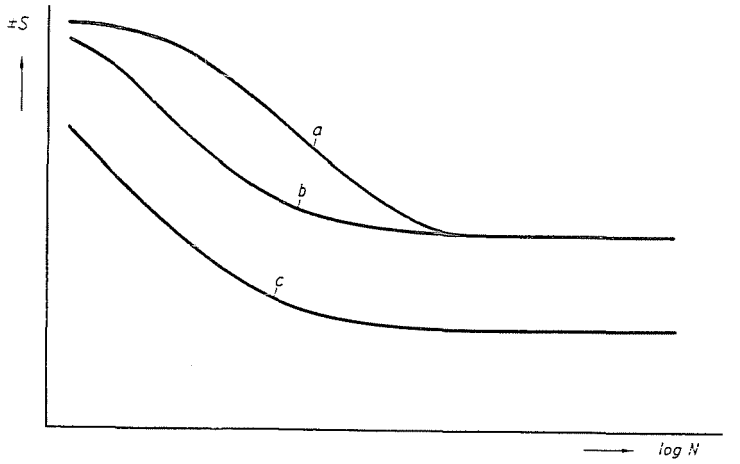

Fig. 8. Fracture development in the high-cycle range (after HEMPEL)
a = fracture line
b = macroscopic crack lines
c = plastic deformation and micro-crack development

line which, however, does not conclude to the fact that this curve would continue to represent a straight line in case of high-cycle fatigue as well. It may be, however, safely stated that the lines indicating fracture and crack spreading commencement, respectively, converge again toward fracture stress point S_f around $N = {}^1/_2 - {}^1/_4$ loading which is in agreement with the fact that, in

course of a simple tensile test, the energy required for the spreading of the crack is negligible when plastic state material types are subject to fracture conditions. At the same time, this figure indicates that the lower the stress level, the higher the cycle number in course of the spreading of the crack. This is, by the way, in full agreement with the results obtained under high-cycle number fatigue conditions [34, 35, 36].

According to HEMPEL et al. [34, 35], high-cycle fatigue phenomena show that in experiments performed near to the endurance limit the traces of plastic deformation can be discovered by means of microscopic methods as soon as with a very low number of loadings. This is followed by the appearance of cracks of either non-spreading [36] or spreading types. The process is schematically illustrated, after [37] by *Fig. 8*.

The low-cycle fatigue phenomena are very similar in nature with the exception, however, that plastic deformation will take place here within each crystallite necessarily as soon as during the first cycle. The results obtained through low-cycle fatigue measurements show a good agreement with the theory by YOKOBORI [38].

6. Origin of the spreading

According to the results of low-cycle fatigue experiments, cracks would start to spread when the energy absorbed by the sample has amounted to a predetermined value characteristic to the material concerned. In subsequent investigations some of the unnotched samples made of the material used for low-cycle fatigue tests have been exposed to fatigue at such a high stress level where the energy absorbed could reach the value of 110 mkp/cm^3 only after a considerable plastic deformation has taken place. With the experiments completed following the absorption of an energy quantity slightly exceeding 110 mkp/cm^3, the cracks could be clearly discovered on the samples.

Subsequently to a pre-fatigue process at lower stress levels where the energy absorbed could not reach the value of 110 mkp/cm^3, the samples were elongated after exposure to the pre-fatigue loading up to the same deformation as that obtained in fatigue tests. Within the latter, the energy produced did not amount to the value of 110 mkp/cm^3 and the samples could not exhibit cracks through a microscopic examination of 250-times magnification, either.

Fig. 9 presents the results of a fatigue test performed at the $S = 100$ kp/mm^2 stress level. By the end of the fourth tensile loading, the sample has absorbed 125 mkp/cm^3 energy. The crack thus developed is illustrated by the figure in a wide open state. The true strain following the fourth tensile load equalled $\varepsilon = 0.26$.

Another sample exposed to repeated loadings at a lower stress level was subject to tensile deformation up to the same true strain value. The total

energy absorbed during the fatigue process and the subsequent tensile loading amounted to 85 mkp/cm³. The microscopic examination of similarly 250-times magnification did not discover any cracks. In order to verify that the initiation of spreading cracks depends on the quantity of absorbed energy characteristic to the material concerned, there have been some simple tensile and compression loadings carried out. MYLONAS et al. [39, 40] pointed out earlier that pre-loading compression, bending, etc. combined with the notching effect would cause brittle fracture. MYLONAS presented his paper summarizing the

Fig. 9. Crack visible following the absorption of an energy amount of 125 mkp/cm³ (250-times magnification)

research results obtained by his working group in this field at the 1964 Prague Conference of the International Institute of Welding [41]. The following paragraphs are quoted verbatim:

"Sufficient precompression at room temperature exhausts the extensional ductility to such an extent as to result in fracture after extensions of the order of 0.01 (1%). The reduction of extensional ductility is not proportional to the amount of precompression. A narrowly determined limit of compressive prestrain exists, the exhaustion limit at which the ductility suffers a rapid reduction. Prestrains smaller than this limit have little effect on the extensional ductility. Larger prestrains cause complete embrittlement."

It is a fact well known long ago that the tensile and compression true stress—true strain curves, respectively, of a material are not congruent *(Fig. 10)*.

In subsequent studies, tensile tests following a single compression loading have been performed. The data on the steel material used for these tests are as follows: yield stress $S_y = 70$ kp/mm², maximum force true stress $S_m = 110$ kp/mm², fracture strain $\varepsilon_f = 0.43$ and absorbed energy per unit

volume in simple tensile tests $W = 49$ mkp/cm^3. Samples were precompressed in such a manner as to have the energy per unit volume absorbed during compression amount to a lesser quantity than 49 mkp/cm^3 in one case and to a higher one in the other. The sample having absorbed under compression conditions an energy amount of 72.5 mkp/cm^3 exhibited, in course of the subsequent tensile test performed at a stress level of $S = 19$ kp/mm^2, a full brittle fracture. Thus the stress bringing about fracture in the tensile test appeared inferior to the virgin yield stress proper.

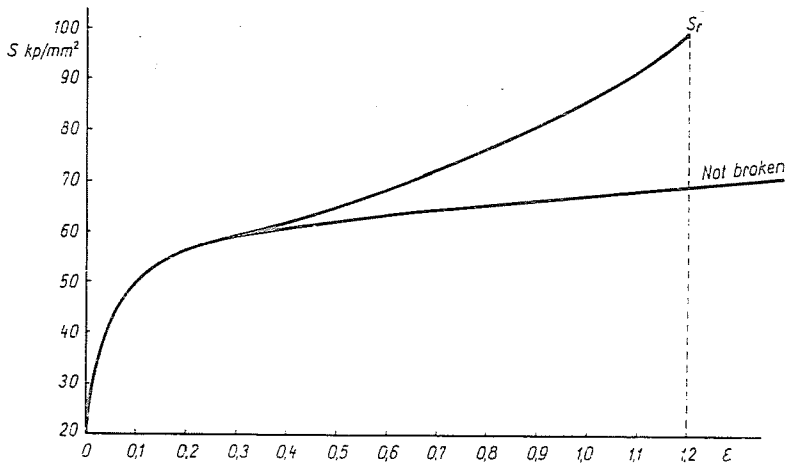

Fig. 10. True stress—true strain curve of a low-carbon steel (C-15) sample in tensile and compression tests, resp.

Another sample having absorbed in course of a deformation process up to a true strain of $\varepsilon = 0.48$ under compression broke at a true strain value of $\varepsilon = 0.19$ in tensile test where the energy absorbed amounted to 10 mkp/cm^3 adding up to a total energy absorbed under tensile as well as compression conditions amounting to 54 mkp/cm^3.

These tensile tests following a single compression loading also reveal that, if the specific energy absorbed in course of the compression test amounts to the value characterizing the material concerned, cracks appear and the sample will break in the tensile test although it could have been compression loaded to a considerable further extent.

7. Conclusions

(1) Axial tension and compression, respectively, initiate a crack spreading in the sample, if the energy absorbed during plastic deformation has amounted to a certain value characteristic to the material tested.

(2) In the simple tensile test, the energy absorbed over the period from the initiation of the crack, that is, from the formation of cavities to full fracture is of an extremely low quantity whereas in a compression test this energy is considerable. In either tensile or compression tests, however, the plastic deformation energy absorbed prior to the appearance of the spreading crack is identical, if the testing conditions are identical.

(3) The energy per unit volume absorbed until whisker fracture is identical to the plastic deformation energy consumed by a very pure metal of identical material type up to the moment of fracture.

(4) The energy produced up to the appearance of the spreading crack in a low-cycle fatigue test performed with constant true stress amplitude is identical to the value determined in the tensile test.

(5) The above statements apply, as expressed in such a simple manner, only to axial tension, compression, or tension and compression loading.

(6) The above statements are not given evidence, as yet, as far as the high-cycle fatigue field is concerned. The statistically identical deformation of all crystallites assumed in low-cycle fatigue tests causing extensive deformations as well as in simple tensile or compression tests, and the energy absorbed by individual crystallites in case of a high-cycle fatigue may differ considerably. In order to clear this latter problem, investigations to extend the fracture criterion described above to the high-cycle fatigue field are under progress.

References

1. YAO, J. T. P. and MUNSE, W. H.: Welding Journal **41**, 183 (1962).
2. COFFIN, L. F.: Appl. Mat. Res. **1**, 129 (1962).
3. PETERSON, R. E.: Fatigue of Metals in Engineering and Design, Edgar Marburg Lecture 1962, ASTM.
4. LIU, S. I., LYNCH, J. J., RIPLING, E. I. and SACHS, G.: Metals Technology (1948) or in PETERSON, R. E.: Fatigue of Metals in Engineering and Design, Edgar Marburg Lecture 1962, ASTM.
5. OROWAN, E.: Welding Journal **31**, 273 (1952).
6. GROSS, J. H. and STOUT, R. D.: Welding Journal **36**, 161 (1955).
7. COFFIN, L. F. and TAVERNELLI, J. F.: Transactions Amer. Inst. M. M. E. **215**, 794 (1959).
8. BALDWIN, E. E., SOKOL, G. J. and COFFIN, L. F.: Proceeding ASTM **57**, 667 (1957).
9. GITTUS, H. J.: Nature **202**, 788 (1964).
10. GILMAN, J. J.: Ref. by KENNEDY, A. J.: Processes of Crepp and Fatigue in Metals, Edinburgh and London, 1962.
11. GILLEMOT, L.: Vorträge des III. Kongresses für Materialprüfung, Budapest. 5, 1964.
12. MARTIN, D. E.: Journal Basic Eng. Trans. A. S. M. E. April. 1961.
13. MARTIN, D. E. and BRINN, J.: Proceedings ASTM **59**, 677 (1959).
14. FELTNER, C. E. and MORROW, J.: T. A. M. Report No 576, Univ. of Illinois, ref. 1, 1959.
15. SCHEVEN, G., SACHS, G. and TONG, K.: Proc. ASTM **57**, 682 (1957).
16. CZOBOLY, E.: Periodica Polytechnica, Engineering **8**, 395 (1964).
17. PRANDTL, L.: Z. Angew. Math. Mech. **8**, 85 (1928).
18. DEUTLER, H.: Z. f. Physik, **33**, 247 (1932).
19. MANJOINE, M. and NÁDAI, A.: Proceedings ASTM **60**, 822 (1940).
20. MANJOINE, M. and NÁDAI, A.: J. Appl. Mech. **8**, A. 77 (1941).
21. GILLEMOT, L. and MIHÁLYI, E.: Vorträge des III. Kongresses für Materialprüfung, Budapest, 269, 1964.

22. GILLEMOT, L.: Archiv. f. Eisenhüttenwesen (in the press).
23. BRIDGEMAN: Studies in Large Plastic Flow and Fracture. Metallurgy and Metallurgical Engineering Series, New York—London, 1952.
24. TRUSZKOWSKY, W.: Bull. de l'Academie Polonaise des Sciences et des Lettres, **1**, 373 (1952).
25. SIEBEL, E. and SCHWAIGERER, S.: Archiv. f. Eisenhüttenwesen **19**, 145 (1948).
26. GILLEMOT, L. and SINAY, G.: Acta Technica Acad. Sci. Hung. **XXII**, 149 (1958).
27. GILLEMOT, L.: Materialprüfung **3**, 330 (1961).
28. OROWAN, E.: Zeitschrift für Physik **89**, 634 (1934).
29. POLÁNYI, M.: Zeitschrift für Physik **89**, 660 (1934).
30. Handbook of Physics, Springer, 1958.
31. GILLEMOT, L.: Freiberger Forschungshefte **B 76**, 5 (1963).
32. BRENNER, S.: J. Appl. Phys. **27**, 1484 (1956).
33. Smithells, Metals Reference Book, London, Butterworths, 1962.
34. WEWER, F., HEMPEL, M., SCHRADER, A.: Archiv f. Eisenhüttenwesen **26**, 739 (1955).
35. HEMPEL, M., SCHRADER, A.: Archiv f. Eisenhüttenwesen **28**, 547 (1957).
36. FROST, N. E. and PHILLIPS, C. E.: Intern. Conf. on Fatigue of Metals. London, 520, 1956.
37. HEMPEL, M.: Materialprüfung **3**, 365 (1961).
38. YOKOBORI, T.: Journal Physical Soc. of Japan **10** (1955).
39. MYLONAS, C.: Welding Journal **40**, 516 (1961).
40. MYLONAS, C., DRUCKER, D. C. and ISBERG, L.: Welding Journal **36**, 9 (1957).
41. MYLONAS, C.: Inst. of Welding, Report IX-419, 1964.

Prof. Dr. László GILLEMOT, Budapest, XI., Bertalan Lajos u. 7. Hungary.